HHS Public Access

Author manuscript

*Neuroscience*. Author manuscript; available in PMC 2022 October 13.

Published in final edited form as:

*Neuroscience*. 2020 August 21; 442: 183–192. doi:10.1016/j.neuroscience.2020.07.006.

# In vivo assessment of cell death and nigrostriatal pathway integrity following continuous expression of C3 transferase

**Rohan. V. Gupta**[1,†], **Angel J. Santiago-Lopez**[1,3,4,†], **Ken Berglund**[1,2], **Robert E. Gross**[1,5,*], **Claire-Anne N. Gutekunst**[1]

[1]Department of Neurosurgery, Emory University School of Medicine, Atlanta, GA

[2]Deptartment of Anesthesiology, Emory University School of Medicine, Atlanta, GA

[3]Interdisciplinary Bioengineering Graduate Program, Georgia Institute of Technology, Atlanta, GA

[4]School of Chemical and Biomolecular Engineering, Georgia Institute of Technology, Atlanta, GA

[5]Wallace H. Coulter Department of Biomedical Engineering, Georgia Institute of Technology, Atlanta, GA

## Abstract

The bacterial exoenzyme C3 transferase (C3) irreversibly inhibits RhoA GTPase leading to stimulation of axonal outgrowth in injured neurons. C3 has been used successfully in models of neurotrauma and shows promise as an option to support cell survival and axonal growth of dopaminergic neurons in Parkinson's disease cell therapy. Whether the continuous expression of C3 in dopaminergic neurons is well-tolerated is unknown. To assess the potential neurotoxicity of sustained expression of C3 in dopaminergic neurons, we generated Cre recombinase-dependent adeno-associated viral vectors (AAV) for targeted C3 delivery to dopaminergic neurons of the mouse substantia nigra pars compacta (SNc). The effect of continuous expression of C3 on dopaminergic neurons was assessed by immunohistochemistry and compared to that of enhanced yellow fluorescent protein (EYFP) as negative controls. We did not find significant reduction of tyrosine hydroxylase expression levels nor the presence of cleaved activated caspase 3. Astrocytic activation as determined by GFAP expression was comparable to EYFP controls. To evaluate the impact of C3 expression on striatal terminals of the nigrostriatal pathway, we compared the rotational behavior of wildtype mice injected unilaterally with either C3 or 6-hydroxydopamine (6-OHDA). Mice injected with C3 exhibited similar ipsiversive rotations to the site of injection in comparison to control mice injected with EYFP and significantly fewer ipsiversive rotations compared to 6-OHDA lesioned mice. Non-significant difference between C3 and EYFP controls in behavioral and histological analyses demonstrate that transduced dopaminergic neurons express

[*]**CORRESPONDENCE :** Claire-Anne N. Gutekunst, PhD, Department of Neurosurgery, Emory University, 101 Woodruff Circle, Woodruff Memorial Research Building, Rm 6337, Atlanta, Georgia 30322, cguteku@emory.edu, Phone: 404-727-1812, Fax: 404-778-4472.

[†]These authors contributed equally to this work.

C3 continuously without apparent adverse effects, supporting the use of C3 in efficacy studies targeting dopaminergic neurons.

## Graphical Abstract

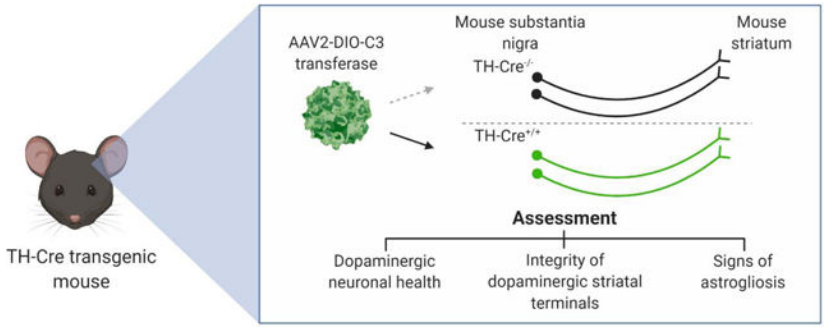


### Keywords

RhoA; C3 transferase; dopaminergic neurons; tyrosine hydroxylase; Cre recombinase; rodent behavior

## INTRODUCTION

Dopaminergic (DA) neurons of the nigrostriatal pathway represent the most vulnerable cell population affecting motor function during the progression of Parkinson's Disease (PD) (Cheng et al., 2010). The need for effective interventions that would restore dopaminergic signaling has motivated the pursuit of dopamine replacement therapies, including gene transfer to increase dopamine metabolism and cell replacement therapy (Elkouzi et al., 2019). Specifically, cell replacement therapy has produced mixed results attributed in part to limited graft survival and innervation of target structures. To overcome these limitations, strategies to provide trophic support have been pursued, such as direct current stimulation and growth factor-infused matrices to support neuronal survival and function (Rowland et al., 2015; Warren Olanow et al., 2015; Wang et al., 2016).

The Rho family of GTPases (RhoA, Rac1, and Cdc42) are key molecular switches responsible for numerous cellular functions including regulating the neuronal actin and microtubule cytoskeleton: Rac1 regulates lamellipodia formation, Cdc42 regulates filopodia, and RhoA regulates axon retraction (Ng et al., 2002; Gross et al., 2007; Stankiewicz and Linseman, 2014). During injuries to the central nervous system (CNS), astrocytic scarring and release of inhibitory glial signals activate the Nogo receptor family, which converge on the activation of RhoA leading to the inhibition of neurite growth and cell death (Dubreuil et al., 2003; McKerracher and Guertin, 2013; Gutekunst et al., 2016).

C3 transferase (C3) is a bacterial exoenzyme derived from *Clostridium botulinum* that irreversibly inhibits RhoA GTPase through ADP ribosylation, stimulating neurite process outgrowth and branching (Lehmann et al., 1999; Gu et al., 2013). Previous studies have shown that RhoA inhibition by C3 promotes axonal regeneration and neuroprotection in

CNS injuries (Boato et al., 2010; Forgione and Fehlings, 2014). Most notably, McKerracher et al. developed a cell permeable C3 variant (Cethrin®) for direct injection to the spinal cord, which promoted extensive axonal sprouting in rodent models of spinal cord injury (McKerracher and Higuchi, 2006; McKerracher and Guertin, 2013). More recently, Rho-independent mechanisms of trophic support have been identified for C3 and C3-derived peptides (Auer et al., 2012). Consistent with these results, our group previously reported that application of C3 to mouse neural stem cells promotes neuronal differentiation and up-regulates pro-survival markers such as p-Akt (Gu et al., 2013).

While the current therapeutic use of C3 focuses on localized delivery of the enzyme, we recently developed C3 expression constructs to provide sustained C3 expression in the CNS when delivered via adeno-associated viral vectors (AAV) (Gutekunst et al., 2016; Santiago-Lopez et al., 2018). Building on these efforts, we sought to elucidate whether the sustained expression of C3 is detrimental to the health of DA neurons. Since the potential use of C3 gene delivery would enable long-term and continuous expression of C3 *in vivo* or *in vitro* in transduced cells prior to intracerebral delivery for PD, we designed our study to assess for signs of transgene toxicity in target dopaminergic cells. Not only is transgene toxicity a general concern for any novel gene therapy, but a recent report on C3 expression in corticostriatal neurons raised potential concerns over the potential of C3 to cause apoptosis in the CNS (Kobayashi et al., 2016).

To better characterize the impact of continuous expression of C3 in DA neurons within their native environment in the nigrostriatal pathway, we used Cre-dependent AAV vectors in conjunction with transgenic mice expressing Cre recombinase under the control of the tyrosine hydroxylase (TH) promoter. Experimentally, our assessment focused on immunohistochemical and stereological determination of DA neuronal health as well as direct evaluation of behavioral performance when comparing C3 to a well-characterized neurotoxin. The outcomes of this study offer *in vivo* validation of whether continuous expression of C3 along the nigrostriatal pathway can be a source of neurotoxicity.

## EXPERIMENTAL PROCEDURES

### Plasmid construction

The DNA plasmid was made using conventional molecular biology with restriction enzymes (RE) and ligases. To generate a viral vector for Cre-dependent expression of C3 (Fig. 1A), the full length C3 cassette with a myc tag following bicistronic, self-cleaving P2A peptide sequence in pAAV/CBA::GFP-P2A-myc-C3 (Custom Cloning Core Division, Emory Integrated Genomics Core) was cut using the BsrGI and BglII RE sites. The product of the digest was then ligated into the BsrGI and AscI sites of pAAV/EF1α::DIO-EYFP (Addgene plasmid #: 27056; a gift from Karl Deisseroth) in the reverse orientation, resulting in pAAV/EF1α::DIO-EYFP-P2A-C3. The incompatible BglII and AscI ends were blunted with Klenow before ligation. The correct subcloning was confirmed by RE digestion analysis and DNA sequencing. The transfection-grade plasmids were produced using a plasmid preparation kit following the manufacturer's instructions (NucleoBond Xtra Midi Plus EF, Macherey-Nagel).

### Cell culture

Human embryonic kidney (HEK) 293T cells were maintained in a humidified 5% $CO_2$ atmosphere at 37 °C in complete medium consisting of Dulbecco's Modified Eagle's medium (DMEM) supplemented with 10% fetal bovine serum, 2 mM L-glutamine, 100 international units (IU)/mL penicillin, and 100 μg/mL streptomycin.

To visualize expression of our cassettes, HEK-293T cells were plated in 10 cm dishes at $8 \times 10^6$ cells per plate and incubated overnight. Cells were transfected with DIO-EYFP or DIO-EYFP-P2A-C3 with or without Cre-IRES-PuroR (Addgene plasmid #: 30205) using calcium phosphate transfection. The following day, cells were imaged using a Leica DMIRE2 inverted fluorescence microscope equipped with a QImaging Retiga EXi CCD camera and Simple PCI acquisition software. Cells were imaged both in brightfield and GFP channels to visualize cell morphology and vector expression.

### AAV vector production

AAV vectors serotyped with AAV2 were prepared by the Emory Viral Vector Core. AAV vectors were packaged using the AAV Helper Free Expression System (Cell Biolabs, Inc., San Diego, CA). The packaging plasmids (pAAV2.2 and pHelper) and transfer plasmid (pAAV/EF1α::DIO-EYFP or pAAV/EF1α::DIO-EYFP-P2A-C3) were transfected into HEK-293T cells using the calcium phosphate method. Medium was replaced 18 hours after transfection with fresh medium, and cells were incubated for an additional 48 hours. Harvested cells were lysed by repeated freezing and thawing, and a crude cell extract containing AAV particles was obtained. AAV viral particles were purified by ultracentrifugation with OptiPrep™ gradient at 200,000 × g for 18 hours with a Beckman VTi 50 rotor followed by 200,000 × g for 40 hours with a Beckman SW 40Ti rotor. The purified particles were dialyzed with phosphate buffered saline (PBS), and then concentrated by ultrafiltration using an Amicon 10K MWCO filter (Merck Milli-pore, Darmstadt, Germany). The copy numbers of the viral genome (vg) were determined by quantitative PCR using the TaqMan Universal Master Mix II (Applied Biosystems, Foster City, CA) with the following primer set and probe: forward primer, 5-CCGTTGTCAGGCAACGTG-3; reverse primer, 5-AGCTGACAGGTGGTGGCAAT-3. PCR was performed in duplicate samples using the Step One real-time PCR system as follows: 95°C for 10 minutes; 40 cycles of 95°C for 15 s and 60°C for 1 minute. The range of the standard curve decided by the dilution series of the transfer plasmid was from $10^5$ to $10^7$ copies. The viral titer was determined to be $1\times10^{12}$ vg/mL for both.

### *In vivo* vector injection

All procedures were conducted in accordance with approved guidelines from the Emory University Institutional Animal Care and Use Committee. C57BL/6J mice (6–12 weeks old, total 19 mice, The Jackson Laboratory, Bar Harbor, ME, USA) were housed in the Emory animal vivarium with a 12-hour light/12-hour dark cycle and *ad libitum* access to food and water. TH::Cre transgenic mice were obtained by crossing hemizygous Tg(TH::Cre) FI12Gsat/Mmucd males from Mutant Mouse Resource and Repository Center (MMRRC stock #: 017262-UCD) with wildtype C57BL/6J female mice. Genotyping was performed on tail tissue from 3-week old pups using a primer pair according to MMRRC.

Stereotactic injection was performed using a pulled glass pipette connected to a microinjector (Nanoject; Drummond Scientific, Bromall, PA, USA) with bouts of 69-nL injections under anesthesia with isoflurane (2–4%, v/v). Two groups of hemizygous TH::Cre mice (n=5 per group) were injected unilaterally with 2 μL (~$2\times10^9$ vg) of either recombinant (r)AAV2/EF1α::DIO-EYFP-P2A-C3 or rAAV2/EF1α::DIO-EYFP in the right SNc (anterior-posterior: −3.1 mm; medial-lateral: −1.6 mm from the bregma; depth: −4.0 mm from the dura) and a third group of TH::Cre-negative littermates (n=5) were injected with rAAV2/EF1α::DIO-EYFP-P2A-C3 in the same location. Since expression of C3 is ultimately controlled by TH-Cre expression via the Cre-Lox system, a 2 μL (~$2\times10^9$ vg) injection was chosen to ensure adequate expression of our construct within the entire SNc. Additionally, a group of wildtype mice (n=4) were injected unilaterally with 2 μL (5.34 μg) of 6-hydroxydopamine (6-OHDA; Sigma–Aldrich, St. Louis, MO, USA), a known neurotoxin to dopaminergic neurons, in 1% (w/v) ascorbic acid in the right striatum (AP: +0.5 mm; DL: −1.7 mm; depth: −3.0 mm) to serve as positive controls for behavioral analysis.

## Behavioral analysis

Mice were assessed for unilateral loss of dopaminergic neurons that could induce rotation behavior at 14- and 28-days post-injection using an automated rotation monitoring system (Rota-Count 8; Columbus Instruments, Columbus, OH). The system records full and partial turning motion of small laboratory animals wearing a harness to which a light and flexible tether has been affixed at one end and to a rotary encoder at the opposite end to monitor the angular direction of the subject. The system monitors both clockwise and counter-clockwise turning behavior, which can be measured using the accompanying software. After harness placement, mice were injected with 2.5 mg/kg of methamphetamine (575 μg/mL in the normal saline; Sigma–Aldrich, St. Louis, MO, USA) intraperitoneally to induce rotation and the number of complete clockwise (ipsiversive) and counterclockwise (contraversive) rotations were measured over a 60-minute period.

## Immunohistochemistry

At the end of the study, mice were deeply anesthetized with a lethal dose of Euthasol (150 mg/kg) injected intraperitoneally, and then perfused intracardially with normal saline (0.9% w/v NaCl), followed by 4% (w/v) paraformaldehyde in 0.1 M phosphate buffer (pH 7.2) for 15 minutes at a rate of 20 mL/minute. Brains were removed and cryoprotected in 30% (w/v) sucrose at 4 °C with subsequent sectioning in the coronal plane at 40 μm thickness using a cryostat followed by collection and rinsing in PBS (pH 7.2).

Free-floating sections were incubated in 0.1% (v/v) TritonX-100 and 3% (w/v) hydrogen peroxide to eliminate endogenous peroxidase, rinsed in PBS, and pre-blocked in 4% (v/v) normal goat serum (NGS) in PBS for 1 hour at room temperature (RT). Sections were incubated in rabbit anti-TH antibody (PelFreez Biologicals, Rogers, AR, USA) in PBS containing 2% NGS at 4 °C for 24 hours, then rinsed and incubated for 1 hour at RT in biotinylated anti-rabbit antibody (ABC Elite; Vector Laboratories, Burlingame, CA, USA) in PBS containing 2% NGS. After several rinses in PBS, the sections were incubated in avidin–biotin complex (ABC Elite; Vector Laboratories, Burlingame, CA, USA) for 90 minutes

at 4 °C. Immunoreactivity was visualized by incubation in 0.05% 3,30-diaminobenzidine tetrahydrochloride (DAB; Sigma, St. Louis, MO, USA) and 0.01% hydrogen peroxide in PBS, until a dark brown reaction product was evident (5–10 minutes). Sections were rinsed and mounted on glass slides, air dried, and coverslipped.

A Leica DM2500 light microscope was utilized in conjunction with Stereologer Version 3.0 CP – Version Two to optically dissect the SNc via the Cavalieri method to count TH-positive neurons. Four SNc sections were selected per animal and software parameters were set to place these sections 10 μm apart in an artificial 40 μm slab. The injected side (IS) and non-injected side (NIS) were analyzed separately and dissection points were selected if they fell within the region of interest. An object with 5x magnification was first used to outline the SNc with the aid of a mouse brain atlas and an object with 40x magnification was then used to select neurons within the field of view.

### Immunofluorescence

To assess expression of C3 in dopaminergic neurons, we examined co-expression of either C3 or TH and the EYFP tag of the viral vector. Free-floating SNc and striatal sections were rinsed in PBS, blocked in 4% NDS and 0.1% Triton-X for 60 minutes at RT, and rinsed in PBS. After rinses in PBS, sections were incubated overnight at 4 °C with either mouse anti-C3 antibody (Courtesy of Lisa McKerracher) or rabbit anti-TH antibody (Pel Freez Biologicals, Rogers, AR, USA) in PBS containing 2% NDS. Sections were rinsed in PBS and incubated in in either Alexa Fluor 594-conjugated donkey anti-rabbit IgG (Jackson Immunoresearch Laboratories, West grove, PA) or Alexa Fluor 594-conjugated donkey anti-mouse IgG (Jackson Immunoresearch Laboratories, West grove, PA, USA) secondary antibody in 2% NDS for 1 hour at RT. Sections were rinsed with PBS, then mounted on glass slides with hard set mounting medium containing the nuclear marker, DAPI (Vectashield; Vector Laboratories, Burlingame, CA, USA). Sections were visualized and imaged using a Zeiss LSM 700 confocal microscope equipped with 405, 488, 555, and 633 nm laser lines.

Intensities of TH in the red channel and EYFP in the green channel were measured with the ImageJ 2.0 software. Fluorescent neurons in each channel were visually counted via the Cell Counter plug-in and merged to identify and count neurons expressing both TH and EYFP. Subsequently, cell bodies were outlined, and area and mean TH and EYFP intensities were measured in the SNc with the aid of a mouse brain atlas. Nuclei were excluded in the TH intensity measurements but were included in those quantifying EYFP intensity.

Immunofluorescence was also utilized to assess cell death through cleaved activated caspase 3 (c-casp 3) and astrocytic activation through glial fibrillary acidic protein (GFAP). Free floating sections were stained with either rabbit anti-c-casp 3 (Cell Signaling Technology, Danvers, MA, USA) or mouse anti-GFAP (Sigma–Aldrich, St. Louis, MO, USA) followed by an Alexa Fluor 594-conjugated donkey anti-rabbit IgG (Jackson Immunoresearch Laboratories, West grove, PA) or Alexa Fluor 594-conjugated donkey anti-mouse IgG (Jackson Immunoresearch Laboratories, West grove, PA, USA) secondary antibody. Sections were visualized as described earlier.

### Statistical analysis

GraphPad Prism 7 software was utilized to analyze the data. Significant deviation from normal distribution in all data sets was tested using a Shapiro-Wilk test. The number of TH-positive neurons between injected and non-injected side exhibited normal distributions and were analyzed using a standard ANOVA for unpaired data and equal variance followed by a post-hoc Tukey multiple comparison test. The TH intensity analysis in transduced neurons within the SNc between EYFP and EYFP-P2A-C3 groups were analyzed using two-sided t-test for unpaired data and equal variance after assumption for normality was met. The number of ipsiversive and contraversive rotations between EYFP, EYFP-P2A-C3 and 6-OHDA groups were analyzed using a Kruskal-Wallis non-parametric test for unpaired data followed by a post-hoc Dunn's multiple comparison since normality was not satisfied. Descriptive statistics are provided as mean ± SEM (* $p < 0.05$, ** $p < 0.01$).

## RESULTS

### Targeted expression of C3 *in vitro* and *in vivo*

The Cre-Lox system utilizes a gene of interest flanked by loxP Cre recombinase (Cre) recognition sites. The gene can be reoriented in a translatable direction in the presence of Cre, whose expression is controlled by a cell type-specific promoter. To assess Cre-dependent expression of C3, HEK-293 cells were plated and transfected with the DIO-EYFP or DIO-EYFP-P2A-C3 transfer plasmid with or without the Cre plasmid. Twenty-four hours after transfection, cellular morphology was visualized on brightfield microscopy, indicating good overall health. As expected, EYFP fluorescence was observed in cells co-transfected with Cre and was absent in cells transfected with C3 alone demonstrating Cre-dependent expression of the vector *in vitro* (Fig. 1B).

Recombinant AAV vectors were produced using these transfer vectors and injected stereotactically into TH::Cre transgenic mice. Fluorescent microscopy revealed EYFP expression in the SNc of TH::Cre transgenic mice injected with DIO-EYFP-P2A-C3 or DIO-EYFP. No EYFP expression was seen in TH::Cre-negative littermates (Fig. 2A). The specific expression of the EYFP tag in the SNc in TH::Cre transgenic mice and its absence in other regions as well as in the SNc of negative mice demonstrated proper targeting of dopaminergic cells with the viral vectors through the Cre-Lox system. Expression of C3 was further confirmed by immunostaining, which co-localized with the EYFP tag, while dopaminergic neurons infected with the control DIO-EYFP vector did not show immunoreactivity against C3 (Fig. 2B).

### Expression of C3 in TH-expressing cells did not induce cell loss or decrease expression of TH

Dopaminergic neurons of the SNc project their axons to striatal neurons of the basal ganglia to form the nigrostriatal pathway. To assess specific expression of C3 in the nigrostriatal pathway, TH staining was performed. The EYFP tag from both the DIO-EYFP-P2A-C3 and DIO-EYFP vectors colocalized with TH immunofluorescence, demonstrating cell-type-specific expression of the Cre-dependent vectors in putative dopaminergic neurons of the SNc (Fig. 3A). Additionally, co-expression of C3 and TH was observed in the striatum,

indicating axonal transport of C3 as dopaminergic cells project from the SNc to the striatum (Fig. 3B). To assess changes in the number of TH-expressing cells, immunohistochemistry with DAB staining and subsequent stereology was performed (Fig. 3C). The numbers of TH-expressing cells in the injected side were not significantly different from those in the non-injected side in either the DIO-EYFP or DIO-EYFP-2A-C3 group (Student's *t*-test; $t(4) = 1.66$, $p = 0.41$, $n = 5$ and 5 for DIO-EYFP and $t(4) = 1.05$, $p = 0.95$, $n = 5$ and 5 for DIO-EYFP-2A-C3; Fig. 3D). Additionally, to evaluate whether C3 had an effect on the expression level of TH, fluorescence intensity was measured in EYFP-expressing cells and it showed no significant difference between the two conditions (Student's *t*-test; $t(4) = 0.90$, $p = 0.51$, $n = 5$ and 5 for DIO-EYFP and DIO-EYFP-2A-C3; Fig. 3E). These findings indicate that expression of TH in dopaminergic neurons was not affected by continuous expression of C3 over the study period.

## Rotation behavior was not significantly affected by C3

Mice underwent amphetamine-induced rotational analysis at 14- and 28-days post-injection with C3 or EYFP vectors. Rotation behavior was compared to mice lesioned with 6-OHDA, a known neurotoxin to dopaminergic neurons, to assess nigrostriatal damage. At 14 days post viral vector injection, mice expressing C3 exhibited a comparable mean number of rotations ipsiversive to the site of injection in comparison to control mice expressing EYFP alone (Kruskal-Wallis test; $p > 0.9999$; $n = 5$). In contrast, mice lesioned with 6-OHDA recorded higher ipsiversive rotations compared to both EYFP (Kruskal-Wallis test; $p = 0.0398$; $n = 5$) and C3 (Kruskal-Wallis test; $p = 0.2332$; $n = 5$) groups. As shown in Fig. 4A, at 14 days post-injection, the DIO-EYFP and DIO-EYFP-P2A-C3 groups exhibited 79% and 60% fewer ipsiversive rotations, respectively, in comparison to mice lesioned with 6-OHDA. These observations were consistent when evaluating behavior at 28 days where the DIO-EYFP and DIO-EYFP-P2A-C3 groups exhibited 66% and 53% fewer ipsilateral rotations, respectively. As shown in Fig. 4B, contraversive rotations (rotations away from the site of injection) showed greater variability in the DIO-EYFP-C3 group with a modest increase in contralateral rotations in comparison to mice lesioned with 6-OHDA at 14 days post-injection (Kruskal-Wallis test; $p = 0.6568$; $n = 5$). These findings suggest the absence of a lesion within the nigrostriatal pathway due to continuous expression of C3 that would induce ipsiversive rotation behavior.

## Continuous expression of C3 did not induce apoptosis or astrogliosis

To assess cell death and astroglial activation in response to continuous expression of C3, immunofluorescence against cleaved caspase 3 (c-casp 3) and GFAP was used, respectively. Dopaminergic neurons expressing EYFP-P2A-C3 or EYFP alone did not show any appreciable caspase 3 activation (Fig. 5A). As for GFAP, expression was seen primarily in the substantia nigra pars reticulata, not in the SNc (Fig. 5B). There was no increase of GFAP expression in the injected side compared to the non-injected side, nor between EYFP-P2A-C3- and EYFP-injected mice. These results suggest that there was no apparent apoptosis or astrogliosis as a result of continuous expression of C3 over our study period.

## DISCUSSION

In the present study, we sought to elucidate whether the sustained expression of C3 is detrimental to the health of dopaminergic (DA) neurons. We investigated the impact of cell type-specific and continuous expression of C3 via Cre-dependent AAV gene delivery within the nigrostriatal pathway. We demonstrated sustained expression of C3 in dopaminergic neurons of the SNc and in their axons within the striatum without apparent neurotoxicity or reactive gliosis over a greater than one month period, allowing further assessment and utilization of this therapeutic approach for applications requiring long-term C3 delivery.

Evaluating the effect of continuous expression of C3 on DA neurons over this time period was necessary as neurotrophic molecules such as C3 are increasingly used in neuroprotective and neurorestorative studies in chronic human disease like PD. Furthermore, a previous report observed caspase 3-dependent cell death and more than 50% loss of mature corticostriatal neurons three weeks after continuous expression of C3 via AAV gene delivery (Kobayashi et al., 2016). In contrast, we did not observe apparent signs of apoptosis or cell loss after continuous expression of C3. These divergent results could be attributed to multiple factors. It is possible that expression of C3 may demonstrate varying effects in different neuronal populations; our study targeted dopaminergic neurons of the SNc, which have not been targeted in previous studies. In addition to cell type-specific differences, potential cell toxicity could be influenced by the specific promoter driving transgene expression. We chose the promoter ef1α as prior studies demonstrated favorable expression of gene constructs under its control in different neuronal cell types. Expression of C3 in Kobayashi et al. (2016) was controlled by the CAGGS promoter, a 1.6-kb hybrid promoter composed of the CMV immediate-early enhance CBA promoter and CBA intron 1/exon 1. The CAGGS promoter is four times stronger than the ef1α promoter utilized in our study, potentially causing increased cell stress and ultimately cell death (Chen et al., 2011). As one of the most extensively studied serotypes, our selection of AAV-2 serotype is generally considered non-toxic as is AAV-DJ, a hybrid AAV used in Kobayashi et al. (2016) that shares 92% homology with AAV-2 (Grimm et al., 2008).

As an additional metric to study the impact of sustained C3 expression on DA neurons in the nigrostriatal system, we analyzed the rotation behavior of unilaterally injected mice and compared it to the behavior of mice injected with 6-OHDA, a neurotoxin that selectively affects DA neurons. Consistent with the absence of signs of cell death, C3 expressing mice did not show behavioral deficits associated with impaired dopaminergic signaling. While we did not quantify dopamine release in the striatum, our rotational behavior analysis can serve as an indirect measure of nigrostriatal integrity since rotational activity correlates with striatal innervation (Boix et al., 2015). Whether C3 expression can be neuroprotective against neurotoxins such as 6-OHDA remains to be investigated. It is possible continuous C3 expression in DA neurons can lead to neuroprotection given previous evidence of anti-axonal degeneration and anti-apoptotic effects of RhoA inhibition (Forgione and Fehlings, 2014; von Elsner et al., 2016). The present study enables such applications of C3 gene therapy since our data shows that sustained C3 expression is not a significant source of toxicity to DA neurons *in vivo* thereby eliminating potential confounding factors in future efficacy studies.

Cell transplant therapies have been long been studied to replace dopaminergic innervation for PD. It is possible to envision a scenario in which autonomous expression of C3 could be used to promote the survival and growth of axons of transplanted embryonic or induced pluripotent stem cell-derived dopaminergic neurons (iPSC-derived DA neurons). iPSC-derived DA neurons have been introduced *in vivo* in rodent and non-human primate PD models (Hargus et al., 2010; Hallett et al., 2015) and more recently in one PD patient (Schweitzer et al., 2020), but the introduction of C3 to this cell population has not yet been considered. The striatum has been a common target for cell transplantation approaches, but cells have been transplanted in the midbrain as well. In the latter studies, it has been demonstrated that transplanted cells show axonal outgrowth along the nigrostriatal pathway (Grealish et al., 2014; Wakeman et al., 2014). Genetic modification of these cells by introducing C3 could augment axonal growth for better innervation and integration in the striatum leading to improved functional outcomes. One caveat of the cell transplant approach is the finding that synuclein aggregates eventually propagate to the transplanted cells, similar to prion transmission (Li et al., 2008; Angot et al., 2012; Masuda-Suzukake et al., 2013). Accumulation of these aggregates leads to significant oxidative stress and ultimately cell death, which will likely affect transplanted neurons. However, RhoA inhibition with C3 has been shown to alleviate synuclein-induced toxicity in DA neurons, and modifying the effect of synuclein-mediated cell stress through identification and inhibition of key molecular targets is therefore necessary for future application of cell transplants (Zhou et al., 2011).

In conclusion, we demonstrated no observable cell death associated with the expression of C3 within dopaminergic neurons of the SNc over a 33-day study period. Targeted delivery of the C3 gene is a promising approach for multiple therapeutic applications including PD. We expect our findings will enable further use of this approach for applications where long-term C3 delivery and continuous expression are needed.

## Acknowledgement:

We thank Kaavya Mandi and Manuel Hazim for their technical help. This work was supported by NIH grants 5T32NS7480-18 (AJS-L), NS085568 (REG), NS079268 (REG), NS079757 (REG), NSF CBET-1512826 (KB/REG) and S10 OD021773 (KB). This study was supported in part by the Emory Integrated Genomics Core (EIGC), which is subsidized by the Emory University School of Medicine and is one of the Emory Integrated Core Facilities. Additional support was provided by the Georgia Clinical & Translational Science Alliance of the National Institutes of Health under Award Number UL1TR002378. The content is solely the responsibility of the authors and does not necessarily reflect the official views of the National Institutes of Health.

## REFERENCES

Angot E, Steiner JA, Tomé CM, Ekström P, Mattsson B, Björklund A, Brundin P (2012) Alpha-synuclein cell-to-cell transfer and seeding in grafted dopaminergic neurons in vivo. PLoS One 7:23–27.

Auer M, Schweigreiter R, Hausott B, Thongrong S, Höltje M, Just I, Bandtlow C, Klimaschewski L (2012) Rho-independent stimulation of axon outgrowth and activation of the ERK and Akt signaling pathways by C3 transferase in sensory neurons. Front Cell Neurosci 6:43 Available at: 10.3389/fncel.2012.00043/abstract. [PubMed: 23087613]

Boato F, Hendrix S, Huelsenbeck SC, Hofmann F, Grosse G, Djalali S, Klimaschewski L, Auer M, Just I, Ahnert-Hilger G, Höltje M (2010) C3 peptide enhances recovery from spinal cord injury

by improved regenerative growth of descending fiber tracts. J Cell Sci 123:1652–1662. [PubMed: 20406886]

Boix J, Padel T, Paul G (2015) A partial lesion model of Parkinson's disease in mice - Characterization of a 6-OHDA-induced medial forebrain bundle lesion. Behav Brain Res.

Chen C, Krohn J, Bhattacharya S, Davies B (2011) A Comparison of Exogenous Promoter Activity at the ROSA26 Locus Using a PhiC31 Integrase Mediated Cassette Exchange Approach in Mouse ES Cells Van Wijnen A, ed. PLoS One 6:e23376 Available at: 10.1371/journal.pone.0023376.

Cheng HC, Ulane CM, Burke RE (2010) Clinical progression in Parkinson disease and the neurobiology of axons. Ann Neurol 67:715–725. [PubMed: 20517933]

Dubreuil CI, Winton MJ, McKerracher L (2003) Rho activation patterns after spinal cord injury and the role of activated Rho in apoptosis in the central nervous system. J Cell Biol 162:233–243. [PubMed: 12860969]

Elkouzi A, Vedam-Mai V, Eisinger RS, Okun MS (2019) Emerging therapies in Parkinson disease — repurposed drugs and new approaches. Nat Rev Neurol 15:204–223 Available at: http://feeds.nature.com/~r/nrneurol/rss/current/~3/T8mt865NVTo/s41582-019-01557?utm_source=researcher_app&utm_medium=referral&utm_campaign=MKEF_USG_Researcher_inbound. [PubMed: 30867588]

Forgione N, Fehlings MG (2014) Rho-ROCK inhibition in the treatment of spinal cord injury. World Neurosurg 82:E535–E539 Available at: 10.1016/j.wneu.2013.01.009. [PubMed: 23298675]

Grealish S, Diguet E, Kirkeby A, Mattsson B, Heuer A, Bramoulle Y, Van Camp N, Perrier AL, Hantraye P, Björklund A, Parmar M (2014) Human ESC-derived dopamine neurons show similar preclinical efficacy and potency to fetal neurons when grafted in a rat model of Parkinson's disease. Cell Stem Cell 15:653–665. [PubMed: 25517469]

Grimm D, Lee JS, Wang L, Desai T, Akache B, Storm TA, Kay MA (2008) In Vitro and In Vivo Gene Therapy Vector Evolution via Multispecies Interbreeding and Retargeting of AdenoAssociated Viruses. J Virol 82:5887–5911. [PubMed: 18400866]

Gross RE, Mei Q, Gutekunst CA, Torre E (2007) The pivotal role of RhoA GTPase in the molecular signaling of axon growth inhibition after CNS injury and targeted therapeutic strategies. Cell Transplant 16:245–262. [PubMed: 17503736]

Gu H, Yu SP, Gutekunst C, Gross RE, Wei L (2013) Inhibition of the Rho signaling pathway improves neurite outgrowth and neuronal differentiation of mouse neural stem cells. Int J Physiol Pathophysiol Pharmacol 5:11–20 Available at: http://www.ncbi.nlm.nih.gov/pubmed/23525456. [PubMed: 23525456]

Gutekunst C-A, Tung JK, McDougal ME, Gross RE (2016) C3 transferase gene therapy for continuous conditional RhoA inhibition. Neuroscience 339:308–318 Available at: http://www.ncbi.nlm.nih.gov/pubmed/27746349. [PubMed: 27746349]

Hallett PJ, Deleidi M, Astradsson A, Smith GA, Cooper O, Osborn TM, Sundberg M, Moore MA, Perez-Torres E, Brownell A-L, Schumacher JM, Spealman RD, Isacson O (2015) Successful Function of Autologous iPSC-Derived Dopamine Neurons following Transplantation in a Non-Human Primate Model of Parkinson's Disease. Cell Stem Cell 16:269–274 Available at: https://linkinghub.elsevier.com/retrieve/pii/S1934590915000569. [PubMed: 25732245]

Hargus G, Cooper O, Deleidi M, Levy A, Lee K, Marlow E, Yow A, Soldner F, Hockemeyer D, Hallett PJ, Osborn T, Jaenisch R, Isacson O (2010) Differentiated Parkinson patient-derived induced pluripotent stem cells grow in the adult rodent brain and reduce motor asymmetry in Parkinsonian rats. Proc Natl Acad Sci 107:15921–15926 Available at: 10.1073/pnas.1010209107. [PubMed: 20798034]

Kobayashi K, Sano H, Kato S, Kuroda K, Nakamuta S, Isa T, Nambu A, Kaibuchi K, Kobayashi K (2016) Survival of corticostriatal neurons by Rho/Rho-kinase signaling pathway. Neurosci Lett 630:45–52 Available at: https://linkinghub.elsevier.com/retrieve/pii/S0304394016305146. [PubMed: 27424794]

Lehmann M, Fournier a, Selles-Navarro I, Dergham P, Sebok a, Leclerc N, Tigyi G, McKerracher L (1999) Inactivation of Rho signaling pathway promotes CNS axon regeneration. J Neurosci 19:7537–7547. [PubMed: 10460260]

Li J-Y, Englund E, Holton JL, Soulet D, Hagell P, Lees AJ, Lashley T, Quinn NP, Rehncrona S, Björklund A, Widner H, Revesz T, Lindvall O, Brundin P (2008) Lewy bodies in grafted neurons in subjects with Parkinson's disease suggest host-to-graft disease propagation. Nat Med 14:501–503 Available at: http://www.ncbi.nlm.nih.gov/pubmed/18391963. [PubMed: 18391963]

Masuda-Suzukake M, Nonaka T, Hosokawa M, Oikawa T, Arai T, Akiyama H, Mann DMA, Hasegawa M (2013) Prion-like spreading of pathological α-synuclein in brain. Brain 136:1128–1138. [PubMed: 23466394]

McKerracher L, Guertin P (2013) Rho as a target to promote repair: translation to clinical studies with cethrin. Curr Pharm Des 19:4400–4410. [PubMed: 23360272]

McKerracher L, Higuchi H (2006) Targeting Rho To Stimulate Repair after Spinal Cord Injury. J Neurotrauma 23:309–317 Available at: 10.1089/neu.2006.23.309. [PubMed: 16629618]

Ng J, Nardine T, Harms M, Tzu J, Goldstein A, Sun Y, Dietzl G, Dickson BJ, Luo L (2002) Rac GTPases control axon growth, guidance and branching. Nature 416:442–447. [PubMed: 11919635]

Rowland NC, Starr PA, Larson PS, Ostrem JL, Marks WJ, Lim DA (2015) Combining cell transplants or gene therapy with deep brain stimulation for Parkinson's disease. Mov Disord 30:190–195. [PubMed: 25521796]

Santiago-Lopez AJ, Gutekunst C-A, Gross RE (2018) C3 transferase gene therapy for continuous RhoA inhibition. In: Rho GTPases, 2nd ed. (Rivero F, ed). Humana Press.

Schweitzer JS et al. (2020) Personalized iPSC-Derived Dopamine Progenitor Cells for Parkinson's Disease. N Engl J Med 382:1926–1932 Available at: 10.1056/NEJMoa1915872. [PubMed: 32402162]

Stankiewicz TR, Linseman D a (2014) Rho family GTPases: key players in neuronal development, neuronal survival, and neurodegeneration. Front Cell Neurosci 8:314 Available at: http://www.pubmedcentral.nih.gov/articlerender.fcgi?artid=4187614&tool=pmcentrez&rendertype=abstract. [PubMed: 25339865]

von Elsner L, Hagemann S, Just I, Rohrbeck A (2016) C3 exoenzyme impairs cell proliferation and apoptosis by altering the activity of transcription factors. Naunyn Schmiedebergs Arch Pharmacol 389:1021–1031. [PubMed: 27351882]

Wakeman DR, Redmond DE, Dodiya HB, Sladek JR, Leranth C, Teng YD, Samulski RJ, Snyder EY (2014) Human Neural Stem Cells Survive Long Term in the Midbrain of Dopamine-Depleted Monkeys After GDNF Overexpression and Project Neurites Toward an Appropriate Target. Stem Cells Transl Med 3:692–701 Available at: 10.5966/sctm.2013-0208. [PubMed: 24744393]

Wang Q, Zuo Z, Wang X, Gu L, Yoshizumi T, Yang Z, Yang L, Liu Q, Liu W, Han Y-J, Kim J-I, Liu B, Wohlschlegel JA, Matsui M, Oka Y, Lin C (2016) Photoactivation and inactivation of Arabidopsis cryptochrome 2. Science (80- ) 354:343 LP – 347 Available at: http://science.sciencemag.org/content/354/6310/343.abstract. [PubMed: 27846570]

Warren Olanow C et al. (2015) Gene delivery of neurturin to putamen and substantia nigra in Parkinson disease: A double-blind, randomized, controlled trial. Ann Neurol 78:248–257 Available at: 10.1002/ana.24436. [PubMed: 26061140]

Zhou Z, Kim J, Insolera R, Peng X, Fink DJ, Mata M (2011) Rho GTPase regulation of α-synuclein and VMAT2: Implications for pathogenesis of Parkinson's disease. Mol Cell Neurosci 48:29–37 Available at: 10.1016/j.mcn.2011.06.002. [PubMed: 21699982]

## HIGHLIGHTS

- Cre adeno-associated vectors (Cre-AAV) enable C3 transferase expression in dopaminergic neurons of the nigrostriatal pathway
- Continuous C3 transferase expression does not lead to observable loss of dopaminergic neurons in the nigrostriatal pathway
- No evidence of astrogliosis was found following continuous C3 transferase expression in the nigrostriatal pathway

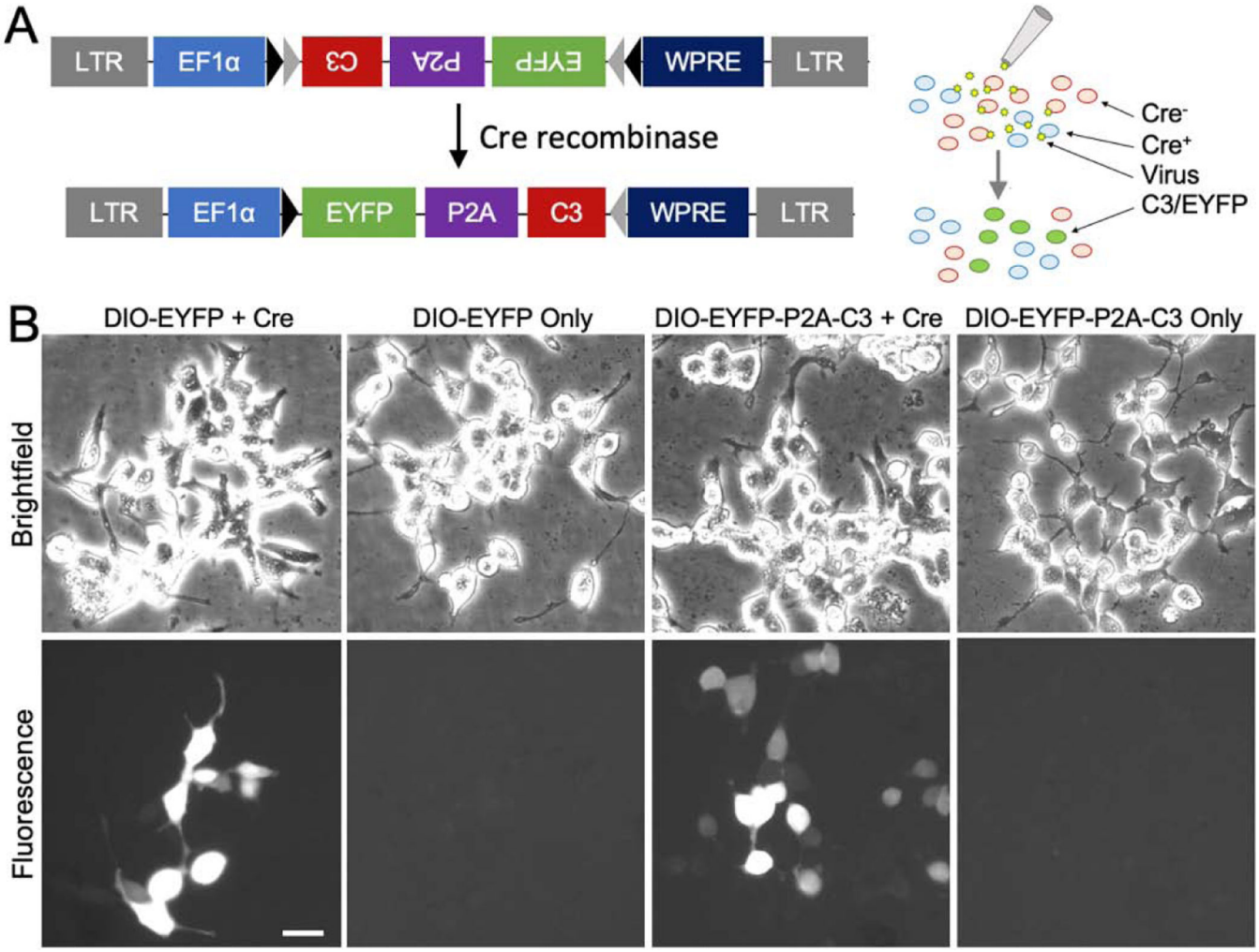


**Figure 1.**

Cre-Lox Expression System for Conditional Expression of C3. (1A) Design of engineered floxed adeno-associated viral (AAV-DIO-Ef1α-EYFP-P2A-C3) vectors for C3 gene delivery for long-term expression in the CNS in a cell-autonomous fashion with utilization of the Cre-Lox system for cell-specific expression. Cells expressing Cre recombinase (Cre) can invert the floxed vectors in the correct reading frame allowing for cell-specific expression. (1B) Brightfield and fluorescent micrographs demonstrating vector expression in the presence of Cre. Vectors were introduced into human embryonic kidney cells (HEK-293) with and without Cre *in vitro*; enhanced yellow fluorescent protein (EYFP) fluorescence was strongly visualized in cells co-transfected with Cre. Scale bar: B) 100 μm.

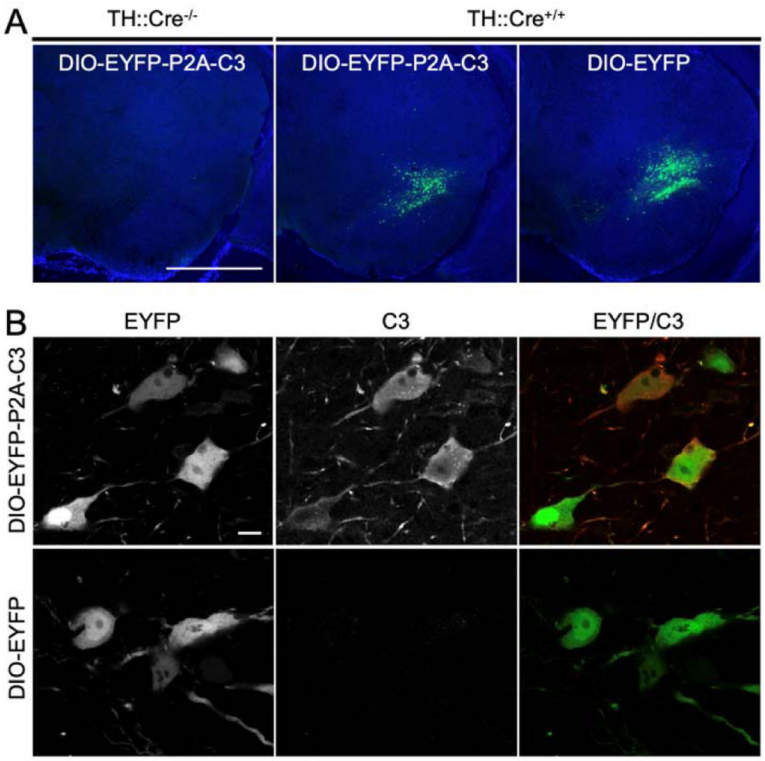


**Figure 2.**

Confirmation of C3 Expression *In Vivo*. (2A) Fluorescent micrographs demonstrating the presence of EYFP in the SNc of TH-Cre$^{+/-}$ mice infected with EYFP-P2A-C3 and those infected with EYFP only. In contrast, EYFP expression was not visualized in TH-Cre$^{-/-}$ mice. The specific expression of EYFP-P2A-C3 and EYFP in the SNc in TH-Cre$^{+/-}$ mice and its absence in other structures including the SNc of TH-Cre$^{-/-}$ mice demonstrated efficacy of the Cre-Lox system for cell-specific vector expression. (2B) Fluorescent micrographs of further C3-specific staining revealing that dopaminergic neurons infected with the floxed vectors containing the EYFP-P2A-C3 cassette were indeed expressing C3 while dopaminergic neurons infected with the EYFP only cassette were not. Scale bars: A) 1 mm; B) 10 μm.

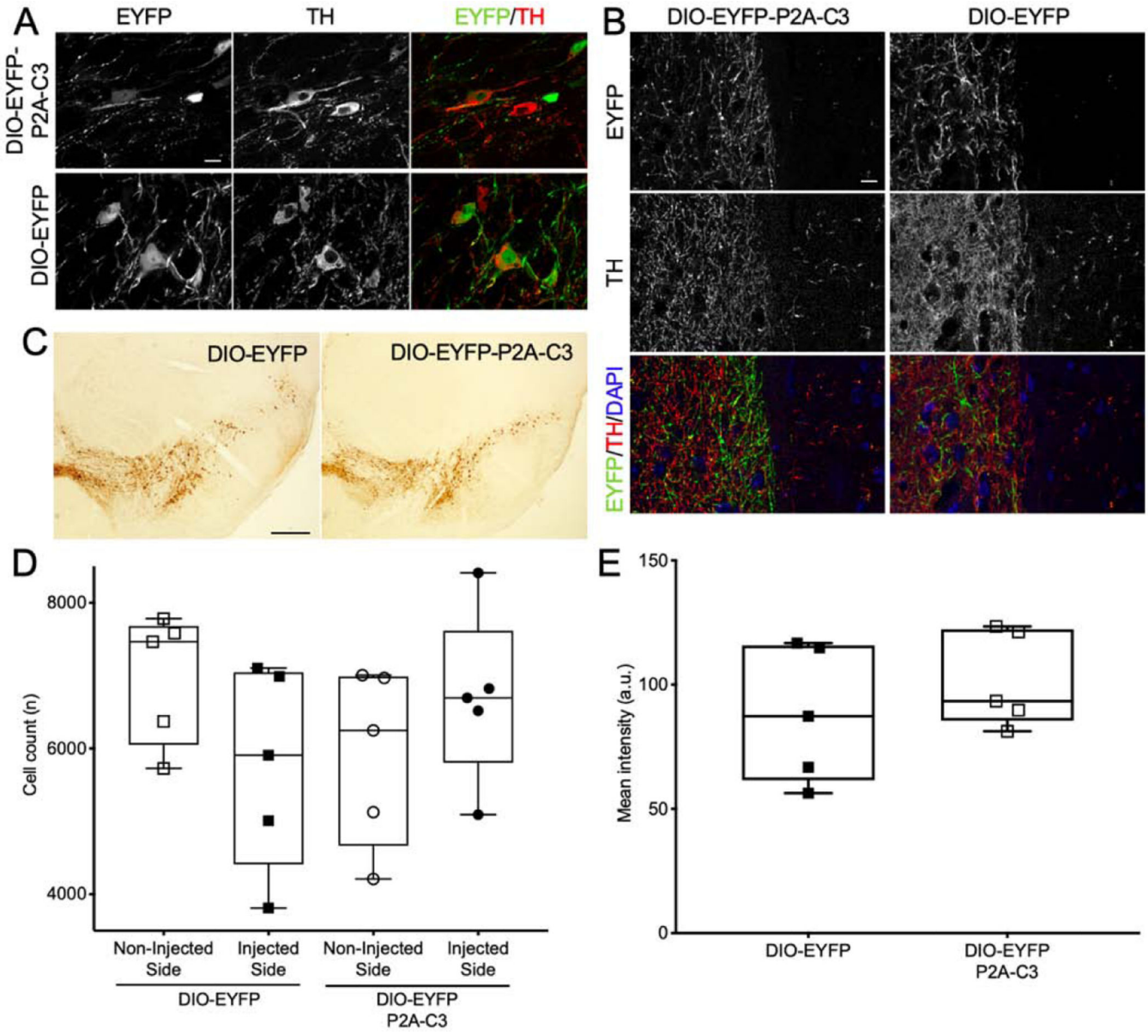


**Figure 3.**

No Significant Decrease in Nigrostriatal TH-Positive Neurons or TH Intensity. (3A) Confocal fluorescent micrographs demonstrating strong TH expression in dopaminergic neurons, which co-localized well with both EYFP-P2A-C3 and EYFP expression, demonstrating cell-specific expression of the floxed vectors in dopaminergic neurons of the SNc. (3B) Micrographs demonstrating expression of both C3 and TH in the striatum, indicating nigrostriatal expression of C3. (3C) TH-DAB-stained SNc sections of mice injected with either DIO-EYFP or DIO-EYFP-C3. (3D) Plot demonstrating no significant difference in mean cell counts compared between the NIS and IS in either the DIO-EYFP (n=5) or DIO-EYFP-2A-C3 (n=5) group. (3E) Plot demonstrating no significant difference in mean TH intensity between the two groups as well. Statistics: t-test. Scale bars: A) 10 μm; B) 0.5 mm; C) 10 μm.

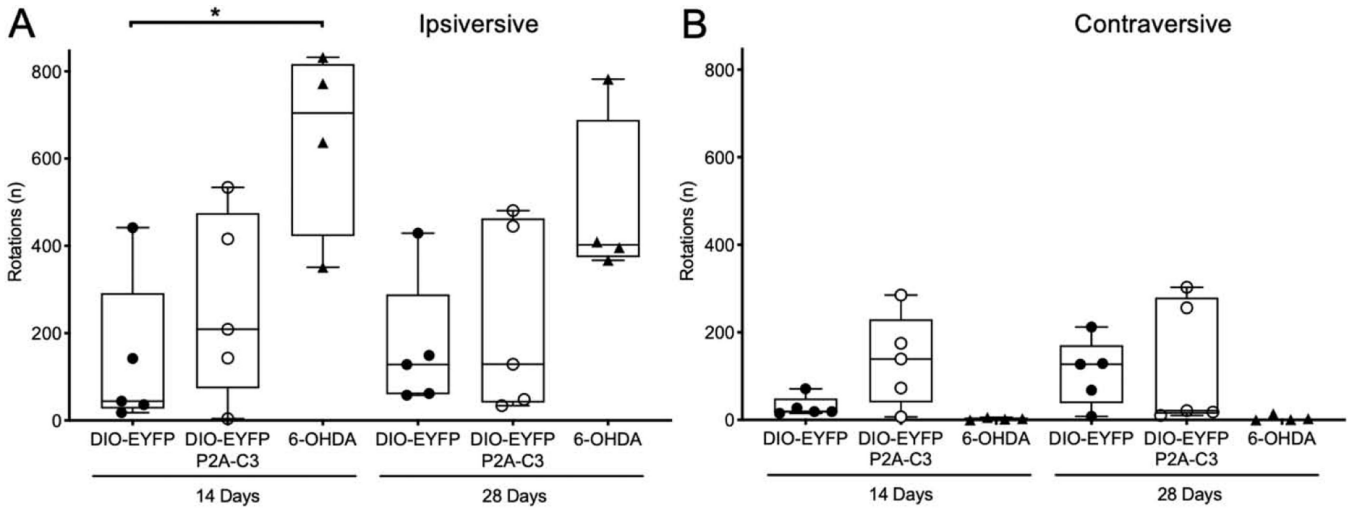


**Figure 4.**

Unilateral C3 expression does not cause a significant increase in amphetamine-induced rotation. (4A) Plot demonstrating mice injected with C3 (n=5) exhibited a similar mean number of rotations ipsiversive to the site of injection in comparison to control mice injected with EYFP alone (n=5) and fewer ipsiversive rotations in comparison to mice lesioned with 6-OHDA (n=4) at 14 days post-injection. (4B) Plot demonstrating greater variability regarding mean number of contraversive rotations away from the site of injection with the DIO-EYFP-C3 group exhibiting more contraversive rotations in comparison to control mice and mice lesioned with 6-OHDA at 14 days post-injection ($p<0.05$). Statistics: Kruskal-Wallis tests with Dunn's multiple comparisons (* $p<0.05$).

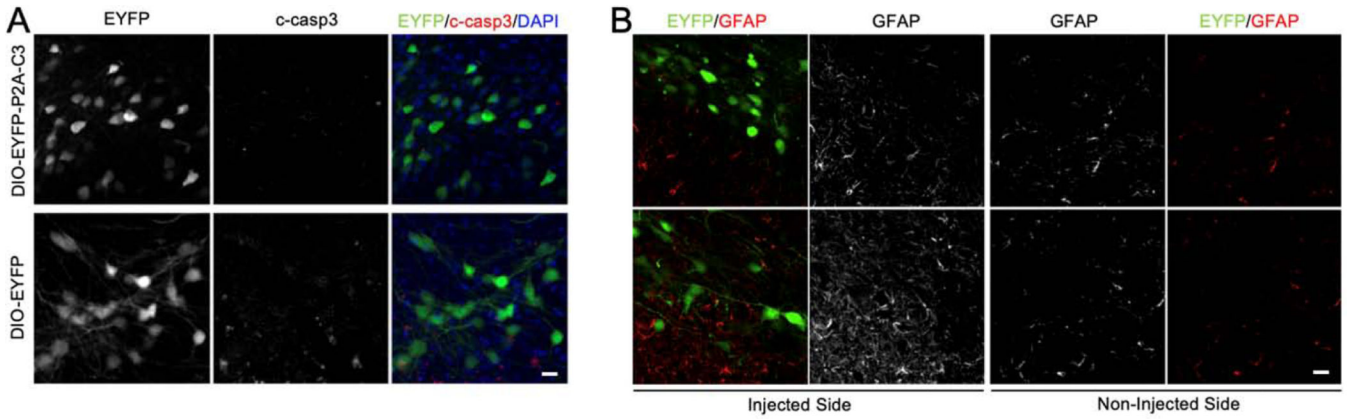


**Figure 5.**

No Increase in Caspase-3 Activation or GFAP Expression. (5A) Confocal fluorescent micrographs demonstrating dopaminergic neurons expressing EYFP-P2A-C3 and EYFP did not show any appreciable caspase 3 activation. (5B) Micrographs demonstrating visualization of GFAP without change in comparison to both controls and non-injected side in each animal. Moreover, expression was seen primarily in the substantia nigra pars reticulata, not in the SNc. Scale bars: A) 10 μm; B) 10 μm.